

A pQCD sized problem in small systems

Isobel Kolbé¹ and W. A. Horowitz¹

¹Department of Physics, University of Cape Town, Private Bag X3, Rondebosch 7701, South Africa

E-mail: isobel.kolbe@gmail.com

Abstract. The Quark Gluon Plasma (QGP) has been studied extensively at the LHC, with jet quenching and particle suppression playing an important role in our ability to characterize this fundamental state of matter. A number of theoretical descriptions concerning the mechanisms whereby particle suppression occurs have been put forward with perturbative methods successfully describing suppression patterns in very central Pb-Pb collisions at the LHC. However, particle suppression is by no means the only hallmark of the existence of the QGP and many measurements at the LHC of smaller colliding systems, such as peripheral Pb-Pb and central p-Pb and p-p, have hinted at the production of a droplet of QGP in alarmingly small volumes. In stark contrast, existing perturbative Quantum Chromodynamical methods rely heavily on the assumption that the system under consideration is large, demanding an extension of pQCD methods to smaller systems. We present precisely such an extension and find corrections on the order of 100% at high energies, revealing a number of shortcomings and problematic assumptions that are present even in traditional pQCD energy loss calculations.

1. Introduction

The discovery of a number of Quark Gluon Plasma (QGP) signals (such as collective behavior [1], strangeness enhancement [2,3], and quarkonium suppression [4]) in small colliding systems such as proton or deuteron collisions with heavy nuclei ($p/d + A$) or even proton-proton (pp) collisions has prompted a vigorous investigation into the properties of such colliding systems. Many of the observed signals are traditionally (that is, in heavy ion collisions) attributed to the presence of a QGP and have been used to characterize the QGP. In particular, jet quenching and particle suppression provided powerful femtoscopic probes of the dynamics of the degrees of freedom of the QGP.

The success of jet tomography is rooted in its successful description by a number of perturbative Quantum Chromodynamical (pQCD) energy loss models [5–8] that are able to qualitatively describe the momentum dependence and angular distribution of the suppression of high-momentum, $\sim 5 - 150$ GeV single particle pions [9,10] and charged hadrons [11–13] from primordial hard light flavors and gluons and electrons [14–16] as well as D [17] and non-prompt J/ψ mesons [18] from open heavy flavor decays at mid rapidity in A+A systems from $\sqrt{s} = 0.2$ TeV to 2.76 TeV.

However, *all* of the standard pQCD energy loss models make the explicit assumption that the QGP system is large [19], calling into question their applicability to the very small systems that must be present if a QGP is created in small colliding systems. In the standard opacity expansion developed by Djordjevic, Gyulassy, Levai and Vitev (DGLV) [20,21], the large system assumption amounts to an assumption that the separation distance $\Delta z \equiv z_1 - z_0 \gg \lambda_{mfp} \gg 1/\mu_D$ between



the initial production position z_0 of the hard parent parton and the position z_1 where it scatters off a QGP medium quasi-particle is large.

In order to apply DGLV energy loss to small systems, we derive the $N = 1$ opacity generalization for all separation distances. We find two curious results:

- (i) Due to the large formation time assumption, only two of the relevant diagrams have non-zero corrections to the standard DGLV result.
- (ii) The (negative) correction terms dominate even for relatively large system sizes at high parent parton energies.

It has been known for some time that all energy loss formalisms are sensitive to the collinear approximation [22,23], but we will demonstrate that the present sensitivity to the large formation time approximation is both new and different.

2. Setup

We follow the DGLV calculation [21], treating the high- p_T eikonal parton produced at an initial point (t_0, z_0, \mathbf{x}_0) inside a finite QGP, where we have used \mathbf{p} to mean transverse 2D vectors, $\vec{\mathbf{p}} = (p_z, \mathbf{p})$ for 3D vectors and $p = (p^0, \vec{\mathbf{p}}) = [p^0 + p^z, p^0 - p^z, \mathbf{p}]$ for four vectors in Minkowski and light cone coordinates respectively. The full calculation is available at [24]. As in the DGLV calculation, we consider the target to be a Gyulassy-Wang Debye screened potential [25] with Fourier and color structure given by

$$\begin{aligned} V_n &= V(\vec{\mathbf{q}}_n) e^{-i\vec{\mathbf{q}}_n \cdot \vec{\mathbf{x}}_n} \\ &= 2\pi\delta(q^0) v(\mathbf{q}_n, q_n^z) e^{-i\vec{\mathbf{q}}_n \cdot \vec{\mathbf{x}}_n} T_{a_n}(R) \otimes T_{a_n}(n). \end{aligned} \quad (1)$$

The color exchanges are handled using the applicable $SU(N_c)$ generator $T_a(n)$ in the d_n dimensional representation of the target or $T_a(R)$ in the d_R dimensional representation of the high- p_T parent parton.

In light cone coordinates the momenta (defined in Figure: 1) of the emitted gluon, the final high- p_T parton, and the exchanged medium Debye quasi-particle are

$$k = \left[xP^+, \frac{m_g^2 + \mathbf{k}^2}{xP^+}, \mathbf{k} \right], p = \left[(1-x)P^+, \frac{M^2 + \mathbf{k}^2}{(1-x)P^+}, -\mathbf{k} \right], q = [q^+, q^-, \mathbf{q}], \quad (2)$$

where the initially produced high- p_T particle of mass M has large momentum $E^+ = P^+ = 2E$ and negligible other momentum components. Notice that we include the Ter-Mikayelian plasmon effect with an effective emitted gluon mass m_g [21,26].

A shorthand for energy ratios will prove useful notationally. Following [21], we define $\omega \approx xE^+/2 = xP^+/2$, $\omega_0 \equiv \mathbf{k}^2/2\omega$, $\omega_i \equiv (\mathbf{k} - \mathbf{q}_i)^2/2\omega$, $\omega_{(ij)} \equiv (\mathbf{k} - \mathbf{q}_i - \mathbf{q}_j)^2/2\omega$, and $\tilde{\omega}_m \equiv (m_g^2 + M^2 x^2)/2\omega$.

Additionally, a number of crucial assumptions are made in line with [21]: 1) the eikonal, or high energy, approximation, for which E^+ is the largest energy scale of the problem; 2) the soft (radiation) approximation $x \ll 1$; 3) collinearity, $k^+ \gg k^-$; 4) that the impact parameter varies over a large transverse area; and, most crucially for the present work, 5) the large formation time assumption $\omega_i \ll \mu_i$, where $\mu_i^2 \equiv \mu^2 + \mathbf{q}_i^2$. These assumptions allow us to 1) (eikonal) ignore the spin of the high- p_T parton; 2) (soft) assume the source current for the parent parton varies slowly with momentum $J(p - q + k) \approx J(p + k) \approx J(p)$; 3) (collinearity) complete a separation of energy scales

$$E^+ \gg k^+ \gg k^- \equiv \omega_0 \sim \omega_{(i\dots j)} \gg \frac{(\mathbf{p} + \mathbf{k})^2}{P^+}; \quad (3)$$

and 4) take the ensemble average over the phase factors, which become $\langle e^{-i(\mathbf{q}-\mathbf{q}')\cdot\mathbf{b}} \rangle = ((2\pi)^2/A_\perp)\delta^2(\mathbf{q}-\mathbf{q}')$.

Within the above setup, we re-evaluated the $N = 1$ in opacity diagrams without the large separation distance $\Delta z \gg 1/\mu$ assumption.

3. Calculation and Results

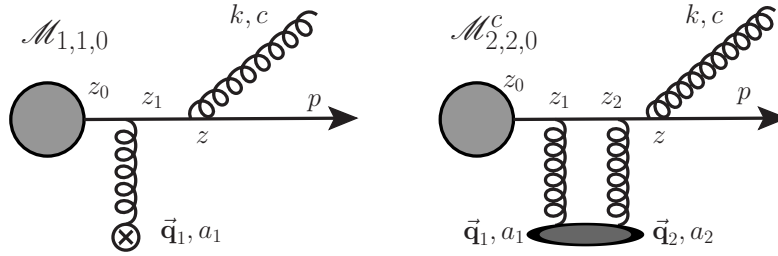


Figure 1: $\mathcal{M}_{1,1,0}$ (left panel) and $\mathcal{M}_{2,2,0}^c$ (right panel) are the only two diagrams that have non-zero short separation distance corrections in the large formation time limit. $\mathcal{M}_{2,2,0}^c$ is the double Born contact diagram, corresponding to the second term in the Dyson series in which two gluons are exchanged with the single scattering center.

Implementing the relaxation of the large separation distance assumption, $\Delta z \gg 1/\mu_D$, amounts to the retention of terms proportional to $\exp(-\mu_D \Delta z)$, that were neglected in the original evaluation of the $N = 1$ in opacity energy loss derivation. Curiously, the large radiated gluon formation time approximation $\omega_i \ll \mu_i$ leads to a tremendous simplification; all but 2 of the 10 diagrams' 18 new small distance correction pole contributions are suppressed under the large formation time assumption in addition to being suppressed under the large separation distance assumption (the relaxation of which is the object of the present calculation). It should be noted that the large formation time assumption allows one to neglect terms in both the original DGLV and the current short separation distance correction. Fig. 1 shows the two diagrams that contribute non-zero small separation distance, large formation time terms to the result.

The full result for these two amplitudes under our approximation scheme is then

$$\mathcal{M}_{1,1,0} \approx -J(p)e^{ipx_0}2gT_{a_1}ca_1 \int \frac{d^2\mathbf{q}_1}{(2\pi)^2} v(0, \mathbf{q}_1) e^{-i\mathbf{q}_1 \cdot \mathbf{b}_1} \times \frac{\mathbf{k} \cdot \boldsymbol{\epsilon}}{\mathbf{k}^2 + m_g^2 + x^2 M^2} \left[e^{i(\omega_0 + \tilde{\omega}_m)(z_1 - z_0)} - \frac{1}{2} e^{-\mu_1(z_1 - z_0)} \right] \quad (4)$$

$$\mathcal{M}_{2,2,0}^c \approx J(p)e^{i(p+k)x_0} \int \frac{d^2\mathbf{q}_1}{(2\pi)^2} \int \frac{d^2\mathbf{q}_2}{(2\pi)^2} e^{-i(\mathbf{q}_1 + \mathbf{q}_2) \cdot \mathbf{b}_1} \times igT_{a_2}T_{a_1}ca_2a_1 v(0, \mathbf{q}_1) v(0, \mathbf{q}_2) \frac{\mathbf{k} \cdot \boldsymbol{\epsilon}}{\mathbf{k}^2 + m_g^2 + x^2 M^2} \times \left[e^{i(\omega_0 + \tilde{\omega}_m)(z_1 - z_0)} + e^{-\mu_1(z_1 - z_0)} \left(1 - \frac{\mu_1 e^{-\mu_2(z_1 - z_0)}}{2(\mu_1 + \mu_2)} \right) \right]. \quad (5)$$

The double differential single inclusive gluon emission distribution is given by [21]

$$d^3N_g^{(1)} d^3N_J = \frac{d^3\vec{\mathbf{p}}}{(2\pi)^3 2p^0} \frac{d^3\vec{\mathbf{k}}}{(2\pi)^3 2\omega} \left(\frac{1}{d_T} \text{Tr} \langle |\mathcal{M}_1|^2 \rangle + \frac{2}{d_T} \Re \text{Tr} \langle \mathcal{M}_0^* \mathcal{M}_2 \rangle \right). \quad (6)$$

From the amplitudes, the energy-weighted integral over the gluon emission distribution $\Delta E = E \int dx x dN_g/dx$ gives the energy loss.

Our main analytic result is then the $N = 1$ first order in opacity small distance generalization of the DGLV induced energy loss of a high- p_T parton in a QGP:

$$\begin{aligned} \Delta E_{ind}^{(1)} = & \frac{C_R \alpha_s L E}{\pi \lambda_g} \int dx \int \frac{d^2 \mathbf{q}_1}{\pi} \frac{\mu^2}{(\mu^2 + \mathbf{q}_1^2)^2} \int \frac{d^2 \mathbf{k}}{\pi} \int d\Delta z \bar{\rho}(\Delta z) \left[-\frac{2(1 - \cos\{(\omega_1 + \tilde{\omega}_m)\Delta z\})}{(\mathbf{k} - \mathbf{q}_1)^2 + m_g^2 + x^2 M^2} \right. \\ & \times \left(\frac{(\mathbf{k} - \mathbf{q}_1) \cdot \mathbf{k}}{\mathbf{k}^2 + m_g^2 + x^2 M^2} - \frac{(\mathbf{k} - \mathbf{q}_1)^2}{(\mathbf{k} - \mathbf{q}_1)^2 + m_g^2 + x^2 M^2} \right) \\ & + \frac{1}{2} e^{-\mu_1 \Delta z} \left\{ \left(\frac{\mathbf{k}}{\mathbf{k}^2 + m_g^2 + x^2 M^2} \right)^2 \left(1 - \frac{2C_R}{C_A} \right) \left(1 - \cos\{(\omega_0 - \tilde{\omega}_m)\Delta z\} \right) \right. \\ & \left. \left. + \frac{\mathbf{k} \cdot (\mathbf{k} - \mathbf{q}_1)}{(\mathbf{k}^2 + m_g^2 + x^2 M^2)((\mathbf{k} - \mathbf{q}_1)^2 + m_g^2 + x^2 M^2)} (\cos\{(\omega_0 - \tilde{\omega}_m)\Delta z\} - \cos\{(\omega_0 - \omega_1)\Delta z\}) \right\} \right]. \end{aligned} \quad (7)$$

The standard DGLV result, with characteristic color triviality, is apparent in the first two lines of 7, while the last two lines are the short separation distance correction. The correction has the expected properties that it vanishes for both large separation distances ($\Delta z \mu_D \ll 1$) and vanishing separation distances (the LPM effect). Our correction term also has a number of surprising features: the term proportional to $2C_R/C_A$ breaks color triviality to all orders in opacity and in fact, although only apparent through numerical analysis, the correction term in fact dominates the original DGLV calculation at high energies.

The numerical investigation of equation (7) is performed following [21] and results in figures 2a, 2b and 2c. The numerical analysis used the following values: $\mu = 0.5$ GeV, $\lambda_{mfp} = 1$ fm, $C_R = 4/3$, $C_A = 3$, $\alpha_s = 0.3$, $m_{charm} \equiv m_c = 1.3$ GeV and $m_{bottom} \equiv m_b = 4.75$ GeV, and the QCD analogue of the Ter-Mikayelian plasmon effect was taken into account by setting $m_{gluon} \equiv m_g = \mu/\sqrt{2}$. As in [26], kinematic upper limits were used for the momentum integrals such that $0 \leq k \leq 2x(1-x)E$ and $0 \leq q \leq \sqrt{3E\mu}$, due to finite kinematics. This choice of k_{max} guarantees that the final momentum of the parent parton is collinear to the initial momentum of the parent parton and that the momentum of the emitted gluon is collinear to the momentum of the parent parton. The fraction of momentum carried away by the radiated gluon, x , was integrated over from 0 to 1. The distribution of scattering centers was assumed to be exponential in order to account for the rapidly expanding medium, $\bar{\rho}(z) = 2 \exp(-2\Delta z/L)/L$.

The fractional energy loss of charm and bottom quarks in a 4 fm long brick of static QGP as a function of parent parton energy is shown in Fig. 2a. Generally, the small distance correction is an energy *gain* in addition to which the correction term increases with energy relative to the DGLV result.

The fractional energy loss of charm and bottom quarks as a function of path length for parent parton with energy $E = 10$ GeV is shown in Fig. 2b. The non-negligible effect for large path lengths of the small separation distance correction is a well understood feature and diminishes with path length.

The most prominent result from our numerical analysis is shown in Fig. 2c. Here, the fractional energy loss of 100 GeV charm and bottom quarks propagating up to 5 fm through a QGP shows clearly that the small distance “correction” term dominates, even out to path lengths of ~ 3 fm, over the leading DGLV result.

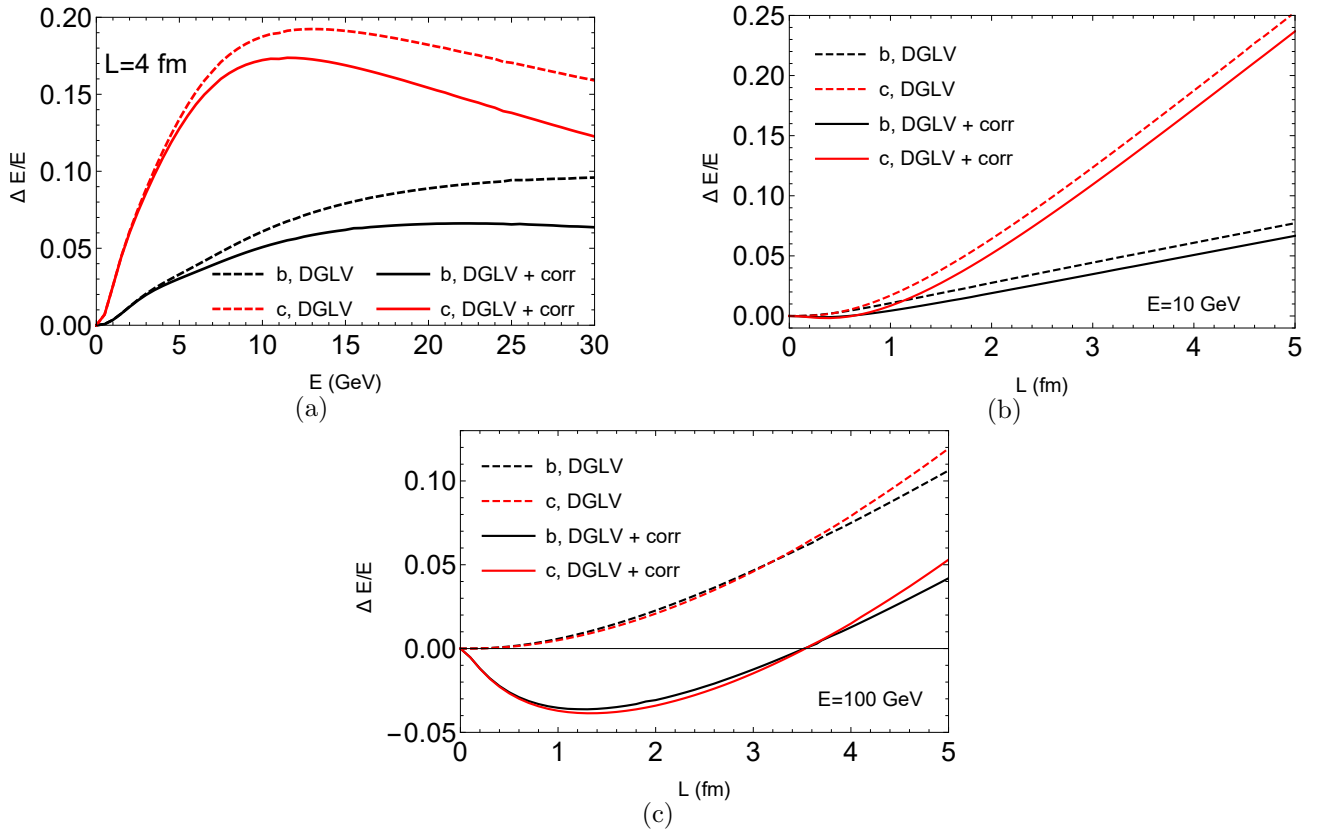


Figure 2: Fractional energy loss of charm and bottom quarks in a QGP with $\mu = 0.5$ GeV and $\lambda_{mfp} = 1$ fm for (a) fixed path length $L = 4$ fm, (b) fixed energy $E = 10$ GeV, and (c) fixed energy $E = 100$ GeV. In the figures, “DGLV” dashed curves are computed from the original $N = 1$ in opacity large separation distance DGLV formula while “DGLV + corr” solid lines are from our all separation distance generalization of the $N = 1$ DGLV result, equation (7).

4. Conclusions

We have performed a short separation distance correction to the standard DGLV calculation and have found that the assumption scheme that results from relaxing the large separation distance assumption breaks down at asymptotically large energies. As such, a more detailed interrogation of the validity of the large formation time assumption in pQCD-based energy loss calculations is necessary.

5. Acknowledgments

The authors wish to thank the SA-CERN Collaboration, the South African National Research Foundation (NRF), and the National Institute for Theoretical Physics (NITheP) for their generous support. The authors also wish to thank CERN for the hospitality extended to them during the completion of part of this work. Finally, the authors wish to thank Miklos Gyulassy, Ulrich Heinz, Sangyong Jeon, and Carlos Salgado for valuable discussions.

References

- [1] V. Khachatryan *et al.*, “Evidence for Collective Multiparticle Correlations in p-Pb Collisions,” *Phys. Rev. Lett.*, vol. 115, no. 1, p. 012301, 2015.
- [2] B. B. Abelev *et al.*, “Multiplicity Dependence of Pion, Kaon, Proton and Lambda Production in p-Pb Collisions at $\sqrt{s_{NN}} = 5.02$ TeV,” *Phys. Lett.*, vol. B728, pp. 25–38, 2014.

- [3] CMS Collaboration, “Multiplicity and rapidity dependence of strange hadrons spectra in pp, pPb, and PbPb collisions at LHC energies,” 2015.
- [4] J. Adam *et al.*, “Centrality dependence of inclusive J/ψ production in p-Pb collisions at $\sqrt{s_{NN}} = 5.02$ TeV,” *JHEP*, vol. 11, p. 127, 2015.
- [5] N. Armesto, M. Cacciari, A. Dainese, C. A. Salgado, and U. A. Wiedemann, “How sensitive are high-p(T) electron spectra at RHIC to heavy quark energy loss?,” *Phys. Lett.*, vol. B637, pp. 362–366, 2006.
- [6] W. A. Horowitz, “Heavy Quark Production and Energy Loss,” *Nucl. Phys.*, vol. A904-905, pp. 186c–193c, 2013.
- [7] K. M. Burke *et al.*, “Extracting the jet transport coefficient from jet quenching in high-energy heavy-ion collisions,” *Phys. Rev.*, vol. C90, no. 1, p. 014909, 2014.
- [8] M. Djordjevic, M. Djordjevic, and B. Blagojevic, “RHIC and LHC jet suppression in non-central collisions,” *Phys. Lett.*, vol. B737, pp. 298–302, 2014.
- [9] A. Adare *et al.*, “Azimuthal anisotropy of π^0 and η mesons in Au + Au collisions at $\sqrt{s_{NN}} = 200$ GeV,” *Phys. Rev.*, vol. C88, no. 6, p. 064910, 2013.
- [10] B. B. Abelev *et al.*, “Neutral pion production at midrapidity in pp and Pb-Pb collisions at $\sqrt{s_{NN}} = 2.76$ TeV,” *Eur. Phys. J.*, vol. C74, no. 10, p. 3108, 2014.
- [11] S. Chatrchyan *et al.*, “Study of high-pT charged particle suppression in PbPb compared to pp collisions at $\sqrt{s_{NN}} = 2.76$ TeV,” *Eur. Phys. J.*, vol. C72, p. 1945, 2012.
- [12] B. Abelev *et al.*, “Centrality Dependence of Charged Particle Production at Large Transverse Momentum in Pb–Pb Collisions at $\sqrt{s_{NN}} = 2.76$ TeV,” *Phys. Lett.*, vol. B720, pp. 52–62, 2013.
- [13] G. Aad *et al.*, “Measurement of charged-particle spectra in Pb+Pb collisions at $\sqrt{s_{NN}} = 2.76$ TeV with the ATLAS detector at the LHC,” *JHEP*, vol. 09, p. 050, 2015.
- [14] B. I. Abelev *et al.*, “Transverse momentum and centrality dependence of high- p_T non-photonic electron suppression in Au+Au collisions at $\sqrt{s_{NN}} = 200$ GeV,” *Phys. Rev. Lett.*, vol. 98, p. 192301, 2007. [Erratum: *Phys. Rev. Lett.* 106, 159902 (2011)].
- [15] S. Sakai, “Measurement of R_{AA} and ν_2 of electrons from heavy-flavour decays in Pb-Pb collisions at $\sqrt{s_{NN}} = 2.76$ TeV with ALICE,” *Nucl. Phys.*, vol. A904-905, pp. 661c–664c, 2013.
- [16] A. Adare *et al.*, “Single electron yields from semileptonic charm and bottom hadron decays in Au+Au collisions at $\sqrt{s_{NN}} = 200$ GeV,” 2015.
- [17] J. Adam *et al.*, “Transverse momentum dependence of D-meson production in Pb-Pb collisions at $\sqrt{s_{NN}} = 2.76$ TeV,” 2015.
- [18] S. Chatrchyan *et al.*, “Suppression of non-prompt J/ψ , prompt J/ψ , and $Y(1S)$ in PbPb collisions at $\sqrt{s_{NN}} = 2.76$ TeV,” *JHEP*, vol. 05, p. 063, 2012.
- [19] U. A. Wiedemann, “Jet Quenching in Heavy Ion Collisions,” pp. 521–562, 2010. [Landolt-Bornstein 23, 521 (2010)].
- [20] M. Gyulassy, P. Levai, and I. Vitev, “Reaction operator approach to nonAbelian energy loss,” *Nucl. Phys.*, vol. B594, pp. 371–419, 2001.
- [21] M. Djordjevic and M. Gyulassy, “Heavy quark radiative energy loss in QCD matter,” *Nucl. Phys.*, vol. A733, pp. 265–298, 2004.
- [22] W. A. Horowitz and B. A. Cole, “Systematic theoretical uncertainties in jet quenching due to gluon kinematics,” *Phys. Rev.*, vol. C81, p. 024909, 2010.
- [23] N. Armesto *et al.*, “Comparison of Jet Quenching Formalisms for a Quark-Gluon Plasma ‘Brick’,” *Phys. Rev.*, vol. C86, p. 064904, 2012.
- [24] I. Kolb  and W. A. Horowitz, “Short path length pQCD corrections to energy loss in the quark gluon plasma,” arXiv:1509.06122.
- [25] M. Gyulassy and X.-n. Wang, “Multiple collisions and induced gluon Bremsstrahlung in QCD,” *Nucl. Phys.*, vol. B420, pp. 583–614, 1994.
- [26] S. Wicks, W. Horowitz, M. Djordjevic, and M. Gyulassy, “Elastic, inelastic, and path length fluctuations in jet tomography,” *Nucl. Phys.*, vol. A784, pp. 426–442, 2007.
- [27] A. Majumder and M. Van Leeuwen, “The Theory and Phenomenology of Perturbative QCD Based Jet Quenching,” *Prog. Part. Nucl. Phys.*, vol. A66, pp. 41–92, 2011.
- [28] A. Adare *et al.*, “Centrality-dependent modification of jet-production rates in deuteron-gold collisions at $\sqrt{s_{NN}} = 200$ GeV,” 2015.
- [29] G. Aad *et al.*, “Centrality and rapidity dependence of inclusive jet production in $\sqrt{s_{NN}} = 5.02$ TeV proton-lead collisions with the ATLAS detector,” *Phys. Lett.*, vol. B748, pp. 392–413, 2015.